Fermi National Accelerator Laboratory

FERMILAB-Conf-89/148-E
[E-741/CDF]

A Missing Transverse Energy Analysis of 1.8 TeV $\bar{p}$ - p Collisions Observed at CDF *

The CDF Collaboration
Reported by J. Freeman
Fermi National Accelerator Laboratory
P.O. Box 500, Batavia, Illinois 60510

June 1989

* Presented at Les Rencontres de Physique de la Vallee d'Aoste: Results and Perspectives in Particle Physics, La Thuile, Italy, February 26-March 4, 1989.

A Missing Transverse Energy Analysis of 1.8 TeV $\bar{p} - p$ Collisions Observed at CDF

The CDF Collaboration
Reported by J. Freeman
Fermi National Accelerator Laboratory

Abstract

We summarize a missing transverse energy analysis of 25.3 nb^{-1} of $\bar{p} - p$ collision data taken with the CDF detector during its 1987 run. With this analysis we excluded supersymmetric squarks of mass less than 73 GeV, and supersymmetric gluinos of mass less than 74 GeV at the 90% CL.

We then present a preliminary missing transverse energy analysis of 1 pb^{-1} of proton-antiproton collision data at c.m. energy of 1.8 TeV observed by the CDF detector during the 1988-1989 Tevatron Collider run. The distribution of events with large missing transverse energy is again found to be consistent with Standard Model expectations. The absence of an excess of events with large missing transverse energy in this preliminary analysis suggests that in the simplest supersymmetry scenario, the existence of supersymmetric squarks of mass less than 150 GeV is unlikely.

1 Introduction

Missing transverse energy ($\not\!\!E_T$) analyses are performed to search for events in which neutrinos or other noninteracting particles are produced. A Standard Model example of such events is W boson production, where the W decays into an electron and neutrino. Exotic sources of large $\not\!\!E_T$ events include production of SUSY squarks or gluinos that decay into quarks and noninteracting photinos, or Leptoquark production where the Leptoquarks decay into quarks and neutrinos.

In this paper we are interested in events with one or more jets associated with $\not\!\!E_T$ (rather than, for instance events with an electron plus $\not\!\!E_T$). After a brief description of the CDF detector, we will summarize backgrounds to the jets + $\not\!\!E_T$ signal. We will then briefly describe a completed analysis of data from the CDF 1987 collider run. Finally we present a preliminary analysis of a subset of data from the 1988-1989 collider run.

2 The CDF Detector

The CDF detector is a fine-grained projective-tower geometry calorimeter covering much of 4π. It is depth-segmented into Electromagnetic (EM) calorimeters followed by hadronic calorimeters. There are three principle subsystems: central scintillator sampling calorimeters with $|\eta|$ <1.0; plug gas sampling calorimeters with 1.0< $|\eta|$ <2.4; and forward gas sampling calorimeters with 2.4< $|\eta|$ <4.2, where η is pseudorapidity, $\eta = -\ln(\tan(\theta/2))$, with θ the polar angle. The tower segmentation is 15° in ϕ, 0.1 in η for the central region, and 5° in ϕ, 0.1 in η for the plug and forward regions.

Inside of the central calorimeters, a superconducting solenoid provides a 15-kG magnetic field for high-precision tracking chambers interior to it. The tracking chambers have $0.2\%\delta P_t/P_t^2$ momentum resolution, and form 3-dimensional tracks with approximately 100 measurements per track. The region of precision tracking extends to roughly $\eta = 1.2$, overlapping nicely the central calorimeter coverage.

A detailed description of the detector is found in Reference [1].

3 Missing Transverse Energy Backgrounds

Many processes can cause events to appear to have $\not\!\!E_T$. Some of the processes we have identified are:

1. cosmic ray showers in the calorimeter in random coincidence with a real $\bar{p}$ − p collision event.

2. a beam-gas event in random coincidence with a real $\bar{p}$ − p collision event. The beam-gas event, with an event vertex far from the detector, can generate large spurious $\not\!\!E_T$.

3. Two $\bar{p}$ − p collision events in the same beam-crossing with separated event vertices. The production vertices of individual photons and π_0's cannot be de-

termined, therefore their E_T cannot be exactly calculated. Depending on the separation of the event vertices and the production angles of the particles, this can be a non-negligible effect. Because the frequency of having two events in the same crossing increases with increasing luminosity, this became an important source of background for the 1988-1989 run.

4. $\bar{p} - p$ events produced far from the center of the detector. For these events, there can be projective holes in the calorimeter, allowing energy to escape detection.

5. QCD multi-jet events where a jet energy is mismeasured because the jet strikes a crack or nonuniform region of the calorimeter, or simply because of the finite energy resolution of the calorimeter.

6. $\bar{p} - p$ events that produce high transverse momentum muons. The muons do not deposit much energy in the calorimeter, and hence generate a $\not\!\!E_T$ signal.

In addition to these sources of spurious $\not\!\!E_T$, there are sources of real $\not\!\!E_T$. They include $W^{\pm} \rightarrow e + \nu$; $W \rightarrow \tau\nu$; high P_t Z's decaying into ν's; and ν's from heavy quark decays.

4 Review of 1987 CDF Analysis

We have recently completed an analysis of data taken in the 1987 $\bar{p} - p$ collider run [2]. The data set for this analysis was $\bar{p} - p$ collisions at 1.8 TeV center-of-mass energy. The two triggers used to collect this data set were a single EM tower trigger with a threshold of 15 GeV, and a E_T sum trigger with a threshold of 45 GeV. The run provided a useful total luminosity of 25.3 nb^{-1} with $\sim 4 \times 10^5$ events which were then filtered by the following requirements:

Cut 1: $\not\!\!E_T$ was required to be larger than 25 GeV.

Cut 2: The highest E_T cluster (clustering was a fixed cone algorithm with radius in $\eta - \phi$ of 0.7) was required to be in the central region of $|\eta|$ <1.0, and to have E_T of at least 15 GeV.

Cut 3: The significance of the $\not\!\!E_T$ of an event is characterized by the quantity $S = \not\!\!E_T / \sqrt{E'_T}$ with the E'_T sum avoiding the forward calorimeters. If calorimeters had pure Gaussian resolution functions, S would be a direct measure of the probability that the $\not\!\!E_T$ of the event was caused simply by measurement fluctuations. Fig. 1 shows the measured S distribution for a set of events with at least one cluster of $E_T > 15$ GeV. To reject $\not\!\!E_T$ events due to calorimeters measurement fluctuations, we required $S > 2.8$.

Cut 4: An $\not\!\!E_T$ signal can arise from mis-measurement of two-jet events due to calorimeters leakage, punch-through, cracks or non-uniform regions. Typically the two jets are separated by 180° in ϕ. We eliminated events with clusters of more than 5 GeV E_T separated by 150° to 210° in ϕ of the highest E_T cluster.

Cut 5: Contamination by cosmic ray showers was eliminated by vetoing events with more than 3 GeV out-of-time E_T in the central hadron calorimeters. The timing window was 20 ns wide centered on the beam-crossing. This cut eliminated cosmic rays in the hadron calorimeters, but accepted >97% of events with high energy jets.

Cut 6: The highest E_T cluster was required to have its EM energy fraction (EMF = cluster EM energy / total cluster energy) in the range 0.2<EMF<0.9. This cut eliminated $W \rightarrow e\nu$ events.

Cut 7: The highest E_T cluster was required to have its charged momentum fraction CHG (CHG is the ratio of the sum of p_T flowing to the cluster (observed by the tracking chambers) divided by the cluster E_T) of CHG > 0.2. This was a requirement that there were charged tracks associated with the cluster. This cut eliminated cosmic ray shower events, where there is in general no central track(s) associated with the shower. Fig. 2 shows a scatter plot of CHG vs. EMF for a set of high E_T jets. We see that the combination of cuts 6 and 7 is very efficient (91%) for high energy jets.

Cut 8: Muons and high transverse momentum minimum-ionizing particles were searched for. If they were observed, the event $\not\!\!E_T$ was corrected for their momenta, and the 25 GeV $\not\!\!E_T$ cut was reimposed.

The $\not\!\!E_T$ distribution for the nine events surviving the cuts is shown in Fig. 3. Two events have $\not\!\!E_T > 30$ GeV, and none have $\not\!\!E_T >40$ GeV.

We estimated the expected number of events with large $\not\!\!E_T$ produced by conventional mechanisms using the ISAJET event generator[3], and a detailed simulation of the CDF detector and hardware trigger. For $\mathcal{L} = 25.3$ nb^{-1} and our set of filtering cuts, for $\not\!\!E_T > 30$ GeV (> 40GeV), we expect 0.9 (0.2) events due to the process $W \rightarrow \tau\nu$; 0.4 (0.2) events due to high P_t Z's decaying into ν's; and 0.2 (0.0) events due to heavy quark decays. The predicted background from conventional mechanisms is in good agreement with our observed $\not\!\!E_T$ distribution.

We then interpreted the absence of an excess of large $\not\!\!E_T$ events to put limits on supersymmetry models.

The SUSY model we considered was a very simple one, with squarks ($\tilde{q}$), gluinos ($\tilde{g}$), and photinos ($\tilde{\gamma}$). We assumed that the six flavors of squarks had the same mass. We assumed that the supersymmetry quantum number R was conserved causing the particles to be pair produced, and causing the lightest SUSY particle to be stable. The lightest particle (hypothesized to be the $\tilde{\gamma}$ in our model) carried away energy, generating the characteristic $\not\!\!E_T$ signature. The decays for different mass combinations of $\tilde{q} - \tilde{g}$ are shown in table 1.

To set limits on SUSY particle production, we ran the ISAJET event generator for various combinations of $\tilde{q} - \tilde{g}$ masses. These MC events were passed through a detector simulation including effects such as cracks, dead areas, finite calorimeters thickness and non-linearities. The trigger criteria and filtering cuts were applied to the events, and the number of surviving events for each combination was tabulated.

Case particle	$m_{\tilde{q}} < m_{\tilde{g}}$	$m_{\tilde{q}} > m_{\tilde{g}}$
$\tilde{q}$ decay	$\tilde{q} \rightarrow q + \tilde{\gamma}$	$\tilde{q} \rightarrow q + \tilde{g}$
$\tilde{g}$ decay	$\tilde{g} \rightarrow g + \tilde{q}$	$\tilde{g} \rightarrow q + \bar{q} + \tilde{\gamma}$

Table 1: SUSY Particle Decay Modes.

We estimated our systematic error in the expected number of events (due to uncertainties in theoretical cross-section, luminosity, and our understanding of the CDF jet response) at ±35%. Using the observation that we saw no event with $\not\!\!E_T > 40$ GeV, we set 90% CL limits on the masses of the SUSY particles. With our systematic uncertainty in the predicted number of events, our 90% CL limit corresponds to the point where we would expect 2.75 events produced by SUSY. We found at the 90% CL, $m_{\tilde{g}} > 73$ GeV, independent of $m_{\tilde{q}}$; similarly, $m_{\tilde{q}} > 74$ GeV, independent of $m_{\tilde{g}}$. Figure 4 shows the limits we found in the $m_{\tilde{q}}$-$m_{\tilde{g}}$ plane. Also shown are earlier limits from the UA1 collaboration [4].

5 Data Reduction 1988-1989 Run

The data set for this analysis was 1 pb^{-1} of $\bar{p} - p$ collisions at 1.8 TeV center-of-mass energy, approximately 1/5 of the full data set for this run. The trigger was a missing transverse energy trigger, with a nominal threshold of 25 GeV. Accompanying the missing E_T requirement was the additional requirement of at least one calorimeter cluster with $|\eta|$ <2.4 and with at least 8 GeV of energy deposition in the EM calorimeter compartment. The presence of a cluster was required to suppress spurious triggers in the gas calorimeters. The true $\not\!\!E_T$ trigger threshold was determined offline by comparison of the trigger decision as a function of calculated $\not\!\!E_T$ for events that were independently triggered. We found that the $\not\!\!E_T$ trigger had high efficiency for jet events with $\not\!\!E_T$ greater than 40 GeV. Our data analysis for this data followed a similar path as that for the 1987 data, with a few differences. We filtered our data by the following requirements:

Cut 1: $\not\!\!E_T > 40$ GeV was required.

Cut 2: We required at least 2 clusters with $E_T > 15$ GeV, and with $|\eta|$ <3.5, and with EMF 0.05 <EMF< 0.90. (An analysis of single cluster events is in progress.)

Cut 3: At least one cluster with $E_T > 15$ GeV was required to be in the central region of $|\eta|$ <1.0, and to have 0.05 <EMF< 0.9. In addition, the cluster was required to have some charged momentum flowing toward the calorimeter energy deposition: CHG > 0.2

Cut 4: The significance S of the $\not\!\!E_T$ was required to be $S > 2.8$.

Cut 5: Events were vetoed if they possessed clusters of more than 5 GeV E_T separated by 150° to 210° in ϕ of the highest E_T cluster.

Cut 6: Events were vetoed if more than 6 GeV E_T was out of time with the $\overline{p} - p$ collision.

Cut 7: To veto the large background of $W^{\pm} \rightarrow e + \nu$, the event was eliminated if it possessed a cluster of $E_T > 15$ GeV with EMF>0.9. This was a crude "electron" veto.

Cut 8: To remove events caused by the coincidence with a beam-gas event with a normal $\overline{p} - p$ collision event, a cut was made on the sum of the longitudinal energy of the event. Figure 5 shows the longitudinal energy distribution for a set of multi-jet events with total $E_T > 100$ GeV. We required the longitudinal energy to be less than 400 GeV. This cut was not 100% effective at removing beam-gas + beam-beam events.

Cut 9: The event vertex was required to have $|Z_{vertex}| < 60$ cm. For events with event vertices larger than this value, the calorimeter hermicity was not guaranteed.

The events surviving this set of cuts were then scanned with the following criteria:

Cut 10: Events with more than 1 primary event vertex (ie two events in the same crossing) were eliminated.

Cut 11: Events with an overlapping beam-gas event were eliminated

Cut 12: Muons and high transverse momentum minimum-ionizing particles were searched for. If they were observed, the event $\not\!\!E_T$ was corrected for their momenta, and the 40 GeV $\not\!\!E_T$ cut was reimposed.

From the 1 pb^{-1} data set, 36 events survived the set of cuts. The $\not\!\!E_T$ distribution for these events is shown in Figure 6

We note that 3 of these events are $W^{\pm} \rightarrow e + \nu$ candidates. These 3 events survived the "electron" veto because of the presence of additional energy deposition within the R=0.7 clustering cone centered about the electron. The additional energy caused the EMF of the cluster be be less than 0.9.

6 Standard Model Backgrounds

We have done a preliminary analysis of expected Standard Model backgrounds. Whenever possible, we have estimated backgrounds using our measured data. When this technique was not possible, we were forced to rely on MonteCarlo. Briefly we will describe the determination of each background.

1. Production of high p_T Z's that then decay into neutrinos. We studied a 2 pb^{-1} sample of $Z \rightarrow e^+ + e^-$. Via software, we eliminated the electrons and then applied our filtering cuts. The surviving events were normalized by the ratio of branching ratios of BR($Z \rightarrow \nu\nu$) / BR($Z \rightarrow e^+e^-$) and corrected for the acceptance of our electron detection. We estimated that this background should produce 8 $\pm$ 5 events.

2. $W \rightarrow e\nu$. The scan of the 36 events in our sample detected 3 candidates of this process. Correcting for our acceptance for the electron identification, we expect 5 $\pm$ 3 events total (including the 3 observed ones).

3. $W \rightarrow \mu\nu$, where the W is produced at high p_T . The scan of our data set found 3 candidates of this process. These 3 events were eliminated by the reapplication of the $\not\!\!E_T$ cut. We estimate that 4 $\pm$ 2 more events have μ's outside our acceptance. These events would remain in our large $\not\!\!E_T$ data set.

4. $W \rightarrow \tau\nu$. We analysed a 2 pb^{-1} set of $W \rightarrow e\nu$ candidates. We replaced the electron cluster by a "tau" cluster where the E_T , EMF and CHG properties of the cluster were determined by Monte Carlo. We applied our filtering cuts and corrected for the electron acceptance. We estimate this background to cause 8 $\pm$ 4 events.

5. Semileptonic heavy quark decays. For this background, we were forced to rely on Monte Carlo predictions. ISAJET events were simulated and passed through our filtering cuts. We estimate this background contributes 9 $\pm$ 4 events.

Table 2 summarizes our estimates for $\not\!\!E_T$ = 40 and 60 GeV. Many of our estimations were limited by poor statistics. An analysis of the complete data set for our 1988-1989 run (about 5 pb^{-1}) will improve these estimates. We see that the rate of high $\not\!\!E_T$ events observed by CDF is consistent with Standard Model expectations.

Background Process	events $\not\!\!E_T$ > 40 Gev	events $\not\!\!E_T$ > 60 GeV
$W \rightarrow e\nu$	5$\pm$3	1$\pm$1
$W \rightarrow \tau\nu$	8$\pm$4	0
$W \rightarrow \mu\nu$	4$\pm$2	0
$Z \rightarrow \nu\nu$	8$\pm$4	4$\pm$3
Heavy Quark Decays	9$\pm$4	3$\pm$1
Total Background	34$\pm$8	8$\pm$3
CDF DATA pb^{-1} Prelim.	36	5

Table 2: Estimated Standard Model background per pb^{-1} passing our filtering cuts.

7 SUSY Implications

We can do a SUSY limit study in a vein similar to our previous work. Sets of Monte Carlo (MC) events with different combinations of ($m_{\tilde{q}}$, $m_{\tilde{g}}$) in the mass range 20-300 GeV were generated with ISAJET, decayed by the prescriptions of table 1, and then simulated. Next our filtering cuts were applied. Table 3 shows results for some of the different mass combinations considered for a integrated luminosity of 1 pb^{-1}.

$(m_{\tilde{q}}, m_{\tilde{g}})$	events $\not\!\!E_T > 40$ Gev	$\not\!\!E_T > 60$ GeV	$\not\!\!E_T > 80$ GeV
(200,80)	69	9.9	0
(200,90)	19	6.3	0
(130,300)	**	10.1	4.9
(140,300)	**	9.1	5.1
(150,300)	**	6.3	3.4
(160,300)	**	8.8	5.9
CDF	36	5	0

Table 3: Expected number of events passing our cuts for combinations of $(m_{\tilde{g}}, m_{\tilde{q}})$. ** → case not considered.

From Table 3, we see that if our model of the properties of SUSY events is correct, we should be sensitive to squark masses of about 150 GeV. We also note that this analysis is not particularly sensitive to the case of $m_{\tilde{q}} > m_{\tilde{g}}$, where there are more jets and less $\not\!\!E_T$ in the final state. The study of this case is in progress.

The simple squark and gluino decay prescriptions of table 1 are expected to be valid for low mass squarks and gluinos. As the masses become larger than O(M_W), this simple decay scenario is no longer thought to remain valid [5]. As the masses increase, new decay mechanisms are allowed, and the $\tilde{g}$ and $\tilde{q}$ do not in general decay directly to the $\tilde{\gamma}$. Rather they decay through cascade decays [6] The cascade decays degrade the $\not\!\!E_T$ signature, but on the other hand open up new signatures such as like-sign di-lepton events. The analysis of these more complex decay scenarios is in progress.

8 Conclusions

A $\not\!\!E_T$ analysis of 25.3 nb^{-1} of $\bar{p} - p$ collision data taken in 1987 found 2 (0) events with $\not\!\!E_T > 30$ (40) GeV. Standard Model backgrounds were estimated to be 1.5 (0.4) events. Using the observation that no event had $\not\!\!E_T > 40$ GeV, we set limits on the masses of supersymmetric particles in a minimal SUSY model. At the 90% confidence level, the mass of the squark must be larger than 73 ± 10 GeV, independent of the mass of the gluino. Similarly, the mass of the gluino must be larger than 74 ± 10 GeV, independent of the mass of the squark.

An extended Tevatron Collider run has taken place during 1988-1989. About 5

pb^{-1} of data have been accumulated. A preliminary analysis of 1 pb^{-1} of data finds that the observed rate of events with $\not\!\!E_T > 40$ GeV and 60 GeV is again consistent with expectations of Standard Model backgrounds. 36 (5) events were observed with $\not\!\!E_T > 40$ (60) GeV. This compares to Standard Model expectations of 34 ± 8 (8 ± 3) events. A complete analysis is in progress.

References

[1] F. Abe *et al.*, NIM **A271** (1988) 387.

[2] F. Abe *et al.*, Phys. Rev. Lett **62** (1989) 1825.

[3] F. Paige and S. Protopopesceau, BNL 38034 (1986).

[4] C. Albajar, *et al.*, Phy. Lett. **198B** (1987) 261.

[5] H. Baer, X. Tata, and J. Woodside, **FSU-HEP-890223**.

[6] H. Baer, J. Ellis, G. B. Gelmini, D. V. Nanopoulos, X. Tata, Phys. Lett. 161B (1985) 175.

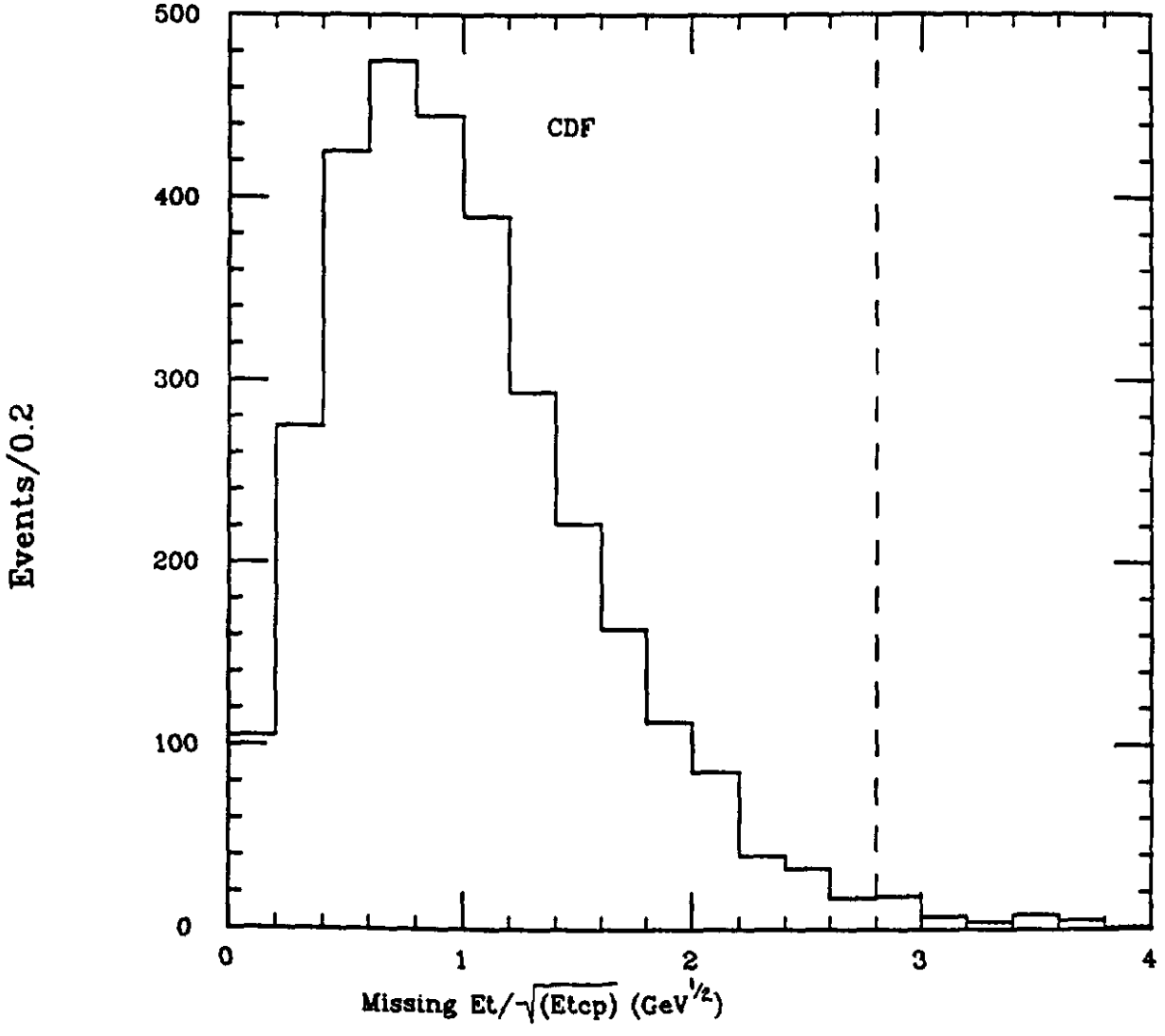

Figure 1: Significance (as defined in the text) distribution for a set of jet events with a jet of $E_T > 15$ GeV. The dashed line at S = 2.8 is the cut described in the text.

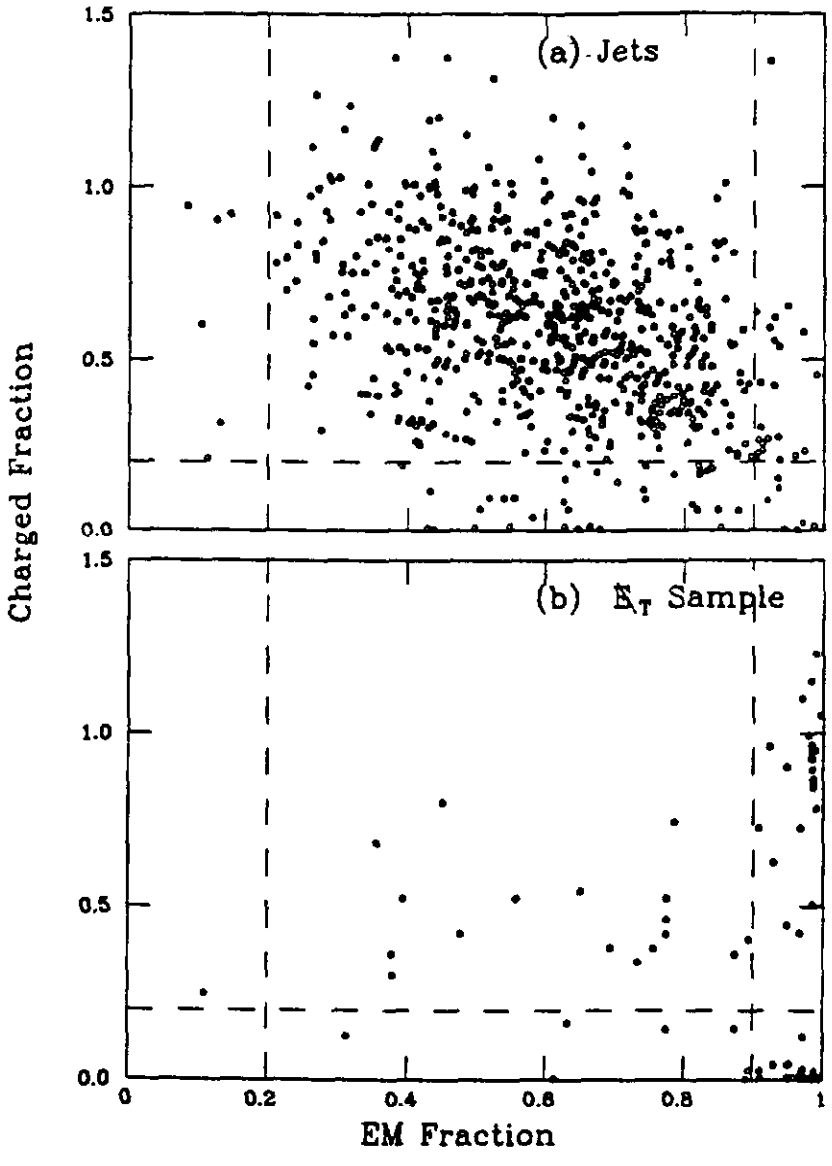

Figure 2: Scatter plot of charged momentum fraction P_T/E_T verses electromagnetic energy fraction (EMF) for (a) high P_T Jets and (b) the missing transverse energy data set. The dashed lines indicate cuts discussed in the text.

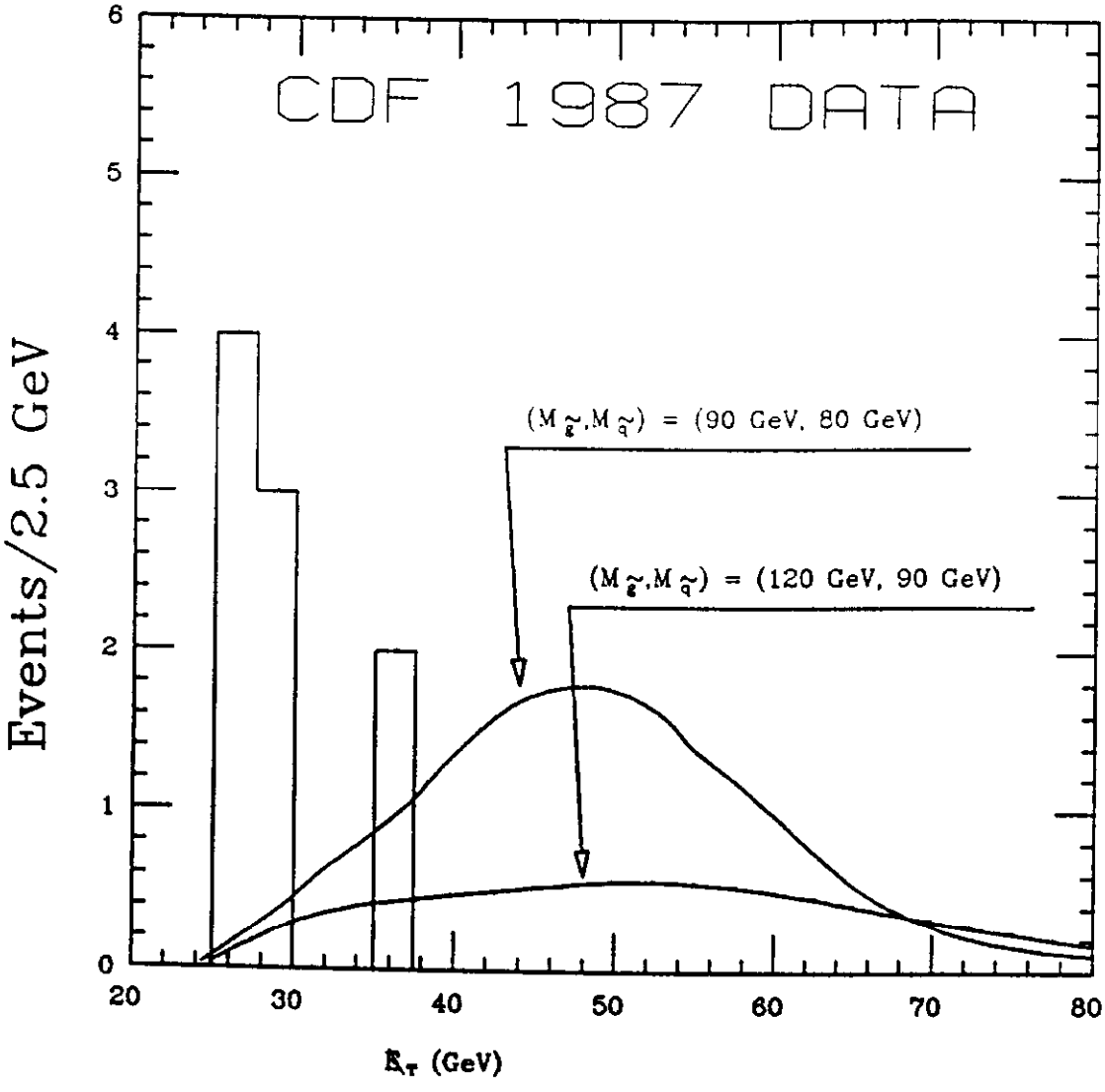

Figure 3: Missing transverse energy distribution for the events surviving cuts, and that expected for two different mass combinations ($m_{\tilde{q}}$, $m_{\tilde{g}}$) in a simple model of supersymmetry. (1987 data set)

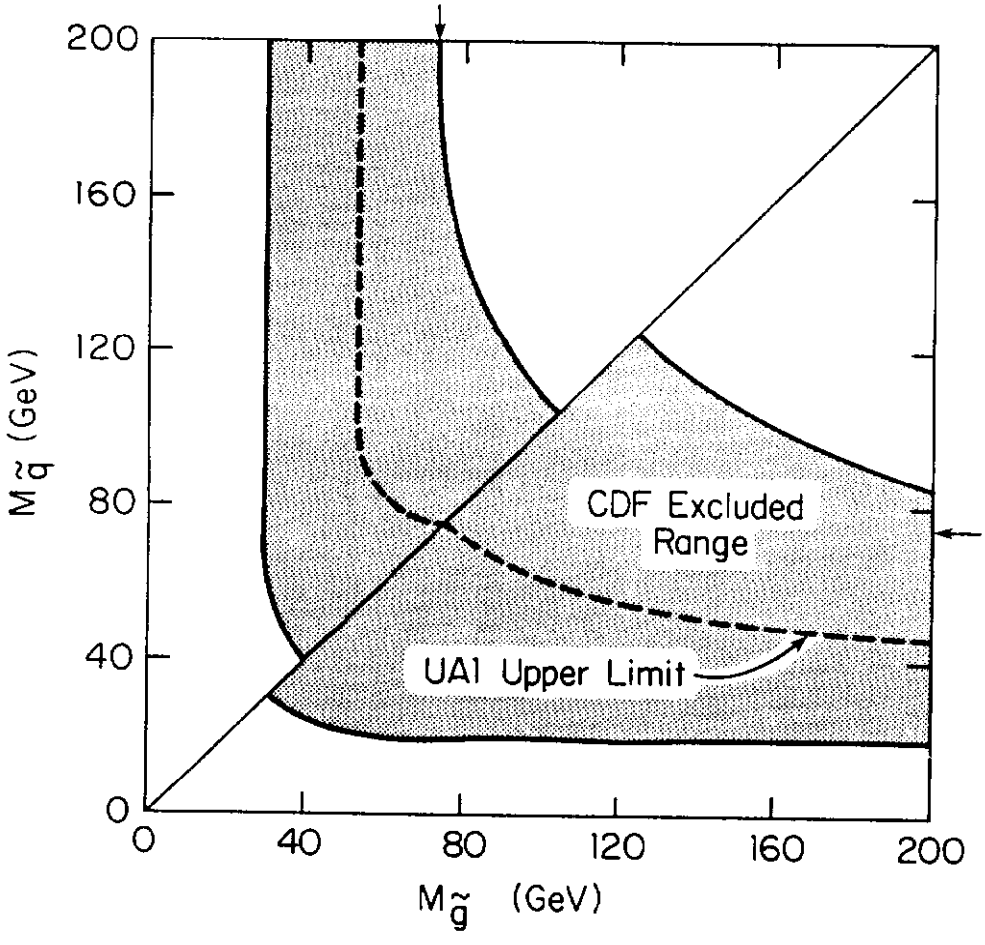

Figure 4: The 90% CL limits in the $m_{\tilde{g}}$, $m_{\tilde{q}}$ plane. The lower solid line is the limit corresponding to a CDF acceptance of 0.1%. Also shown are the limits placed by the UA1 analysis.

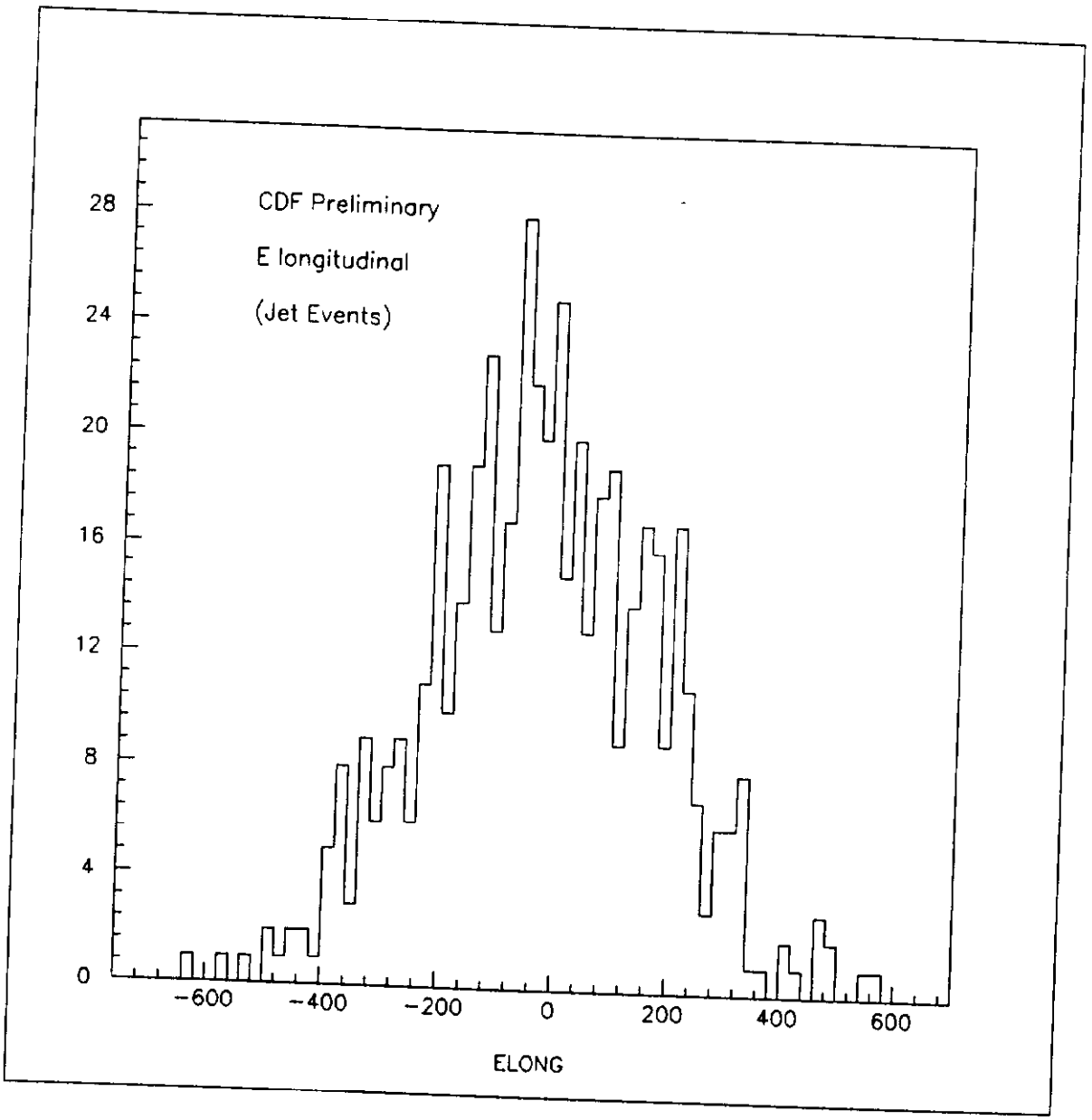

Figure 5: The longitudinal energy distribution for a set of high E_T jet events.

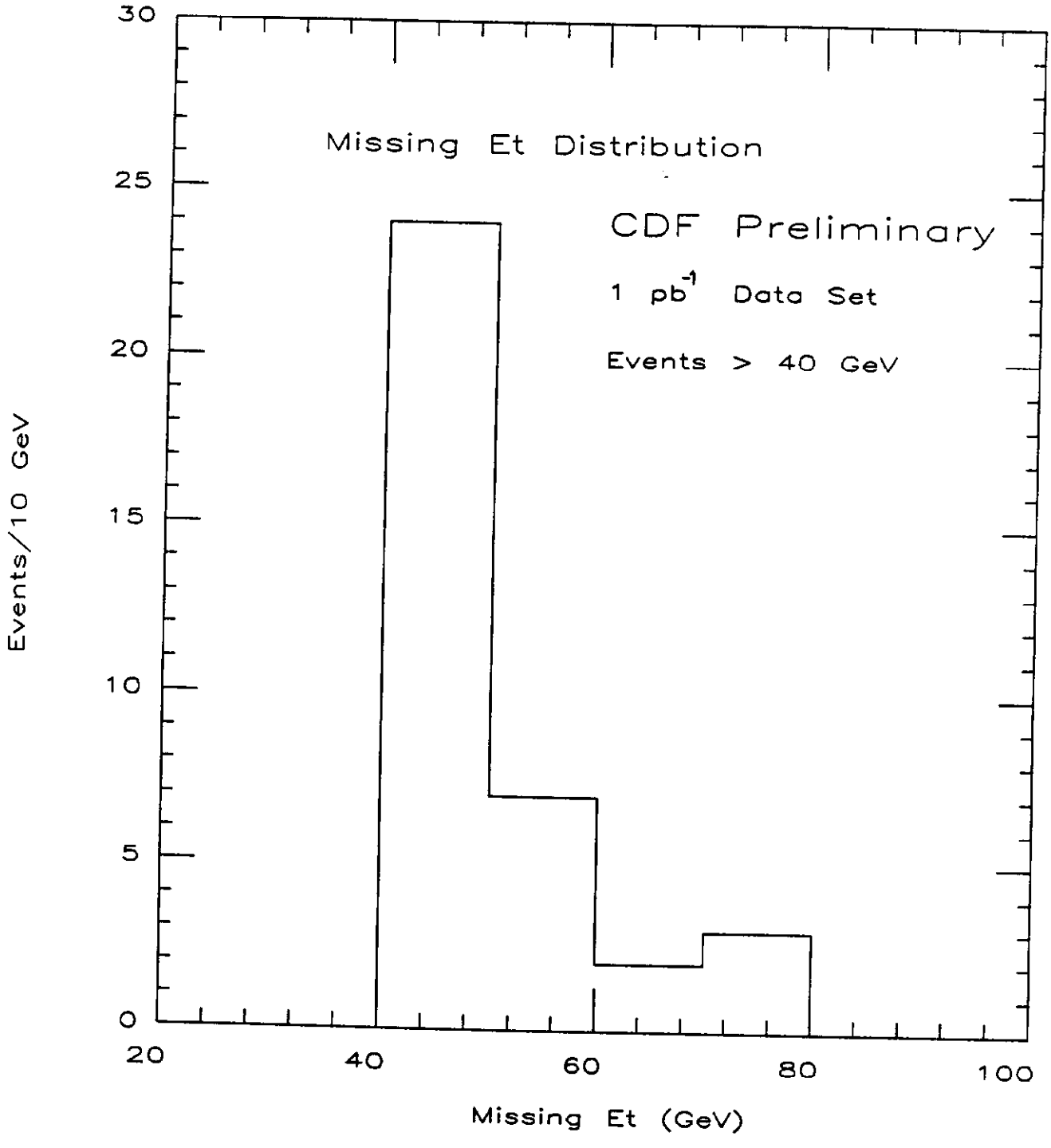

Figure 6: Preliminary missing E_T distribution for events surviving cuts. (1988-1989 data set).